Electronic Supplementary Material (ESI) for Journal of Materials Chemistry C.

The $R_{10}Pd_{21}$ compounds (R = Y, Pr, Nd, Sm, Gd-Lu). Crystal structure and magnetism of the 'RPd_2' phases[§]

Pietro Manfrinetti,[ab]* Alessia Provino,[ab] Nediadath S. Sangeetha[c¥], Sudesh K. Dhar[c]

[a] *Department of Chemistry, University of Genova, Via Dodecaneso 31, 16146 Genova, Italy*

[b] *Institute SPIN-CNR, Corso Perrone 24, 16152 Genova, Italy*

[c] *Condensed Matter Physics & Material Science, Tata Institute of Fundamental Research, Homi Bhabha Road, Mumbai 400 005, India*

[§] Dedicated to the memory of Prof. Karl Gschneidner, Jr.

Electronic Supplementary Information (ESI) available

Supplementary Information contains the Tables of the Rietveld refinement data for the $Nd_{10}Pd_{21}$ (**Table S1**), $Tb_{10}Pd_{21}$ (**Table S2**) and $Lu_{10}Pd_{21}$ (**Table S3**) compounds, the Figures showing: the SEM microphotograph of four samples prepared at the compositions $Sc_{35}Pd_{65}$, $Pr_{10}Pd_{21}$, $Nd_{10}Pd_{21}$ and $Gd_{10}Pd_{21}$ (**Fig. S1**), the trend of the volume contraction *vs.* the R^{3+} ionic radius for the $R_{10}Pd_{21}$ compounds (**Fig. S2**), the Rietveld refinement profile for the $Nd_{10}Pd_{21}$ (**Fig. S3**), $Tb_{10}Pd_{21}$ (**Fig. S4**) and $Lu_{10}Pd_{21}$ (**Fig. S5**) compounds.

Table S1 Rietveld refinement data, with standardized atomic positions, for the $Nd_{10}Pd_{21}$ compound.

Atom	Wyckoff site	Atomic coordinates			Occupation
		x	*y*	*z*	
Nd1	4*i*	0.6496(7)	0	0.021(1)	1
Nd2	4*i*	0.8538(7)	0	0.1459(9)	1
Nd3	4*i*	0.6839(7)	0	0.300(1)	1
Nd4	4*i*	0.0727(7)	0	0.3102(9)	1
Nd5	4*i*	0.1197(6)	0	0.6317(8)	1
Nd6	4*i*	0.2776(8)	0	0.425(1)	1
Nd7	4*i*	0.4303(8)	0	0.513(1)	1
Nd8	4*i*	0.0451(7)	0	0.090(1)	1
Nd9	4*i*	0.4629(9)	0	0.222(1)	1
Nd10	4*i*	0.2372(8)	0	0.148(1)	1
Pd1	4*i*	0.148(1)	0	0.026(1)	1
Pd2	4*i*	0.3559(8)	0	0.166(1)	1
Pd3	4*i*	0.1836(9)	0	0.302(1)	1
Pd4	4*i*	0.5626(8)	0	0.290(1)	1
Pd5	4*i*	0.3825(8)	0	0.334(1)	1
Pd6	4*i*	0.2272(9)	0	0.582(1)	1
Pd7	4*i*	0.0648(9)	0	0.475(1)	1
Pd8	4*i*	0.5382(8)	0	0.095(1)	1
Pd9	4*i*	0.036(1)	0	0.775(1)	1
Pd10	4*i*	0.734(1)	0	0.144(1)	1
Pd11	4*e*	1/4	1/4	0	1
Pd12	8*j*	0.2998(4)	0.246(4)	0.2776(7)	1
Pd13	8*j*	0.1297(4)	0.271(3)	0.1761(6)	1
Pd14	8*j*	0.1658(3)	0.212(2)	0.4552(6)	1
Pd15	8*j*	0.4437(4)	0.254(4)	0.0657(6)	1
Pd16	8*j*	0.4839(4)	0.247(3)	0.3850(6)	1

a = 25.0991(6) Å, b = 5.7929(1) Å, c =16.6395(2) Å, β = 90.7840(4)°

R_B = 1.2 %, R_F = 1.1 %, R_{wp} = 11.5 %, χ^2 = 0.7, B_{over} = 0.428(2) Å^2

Table S2 Rietveld refinement data, with standardized atomic positions, for the $Tb_{10}Pd_{21}$ compound.

Atom	Wyckoff site	Atomic coordinates			Occupation
		x	*y*	*z*	
Tb1	4*i*	0.6470(6)	0	0.0208(8)	1
Tb2	4*i*	0.8545(6)	0	0.1509(9)	1
Tb3	4*i*	0.6872(5)	0	0.3072(8)	1
Tb4	4*i*	0.0762(5)	0	0.3150(7)	1
Tb5	4*i*	0.1182(5)	0	0.6317(7)	1
Tb6	4*i*	0.2770(6)	0	0.4227(8)	1
Tb7	4*i*	0.4313(7)	0	0.5200(9)	1
Tb8	4*i*	0.0422(6)	0	0.0931(8)	1
Tb9	4*i*	0.4695(5)	0	0.2219(8)	1
Tb10	4*i*	0.2369(6)	0	0.1469(9)	1
Pd1	4*i*	0.1487(7)	0	0.022(1)	1
Pd2	4*i*	0.3576(7)	0	0.160(1)	1
Pd3	4*i*	0.1882(6)	0	0.2959(9)	1
Pd4	4*i*	0.5665(6)	0	0.2926(8)	1
Pd5	4*i*	0.3838(6)	0	0.3368(9)	1
Pd6	4*i*	0.2328(7)	0	0.579(1)	1
Pd7	4*i*	0.0638(7)	0	0.482(1)	1
Pd8	4*i*	0.5431(7)	0	0.0946(9)	1
Pd9	4*i*	0.0389(7)	0	0.773(1)	1
Pd10	4*i*	0.7400(8)	0	0.147(1)	1
Pd11	4*e*	1/4	1/4	0	1
Pd12	8*j*	0.2950(3)	0.256(3)	0.2724(6)	1
Pd13	8*j*	0.1283(3)	0.256(3)	0.1759(5)	1
Pd14	8*j*	0.1653(2)	0.229(2)	0.4529(4)	1
Pd15	8*j*	0.4415(3)	0.244(3)	0.0606(5)	1
Pd16	8*j*	0.4837(3)	0.252(2)	0.3837(4)	1

a = 24.5611(6) Å, b = 5.7339(1) Å, c =16.3784(4) Å, β = 91.1349(2)°

R_B = 1.5 %, R_F = 1.5 %, R_{wp} = 8.6 %, χ^2 = 0.8, B_{over} = 2.00(2) Å^2

Table S3 Rietveld refinement data, with standardized atomic positions, for the $Lu_{10}Pd_{21}$ compound; a small amount of Lu_3Pd_5 phase is also present in the sample.

Atom	Wyckoff site	Atomic coordinates			Occupation
		x	*y*	*z*	
Lu1	4*i*	0.6478(4)	0	0.0176(5)	1
Lu2	4*i*	0.8537(4)	0	0.1383(5)	1
Lu3	4*i*	0.6906(4)	0	0.3043(7)	1
Lu4	4*i*	0.0779(4)	0	0.3111(6)	1
Lu5	4*i*	0.1182(4)	0	0.6362(6)	1
Lu6	4*i*	0.2776(4)	0	0.4208(6)	1
Lu7	4*i*	0.4264(4)	0	0.5158(5)	1
Lu8	4*i*	0.0421(4)	0	0.0939(6)	1
Lu9	4*i*	0.4708(4)	0	0.2262(6)	1
Lu10	4*i*	0.2370(4)	0	0.1469(6)	1
Pd1	4*i*	0.1474 (6)	0	0.0310(8)	1
Pd2	4*i*	0.3638(5)	0	0.1664(9)	1
Pd3	4*i*	0.1908(7)	0	0.2998(9)	1
Pd4	4*i*	0.5739(6)	0	0.3071(9)	1
Pd5	4*i*	0.3859(6)	0	0.3428(9)	1
Pd6	4*i*	0.2309(6)	0	0.573(1)	1
Pd7	4*i*	0.0595(5)	0	0.4893(9)	1
Pd8	4*i*	0.5490(6)	0	0.0896(9)	1
Pd9	4*i*	0.0357(7)	0	0.778(1)	1
Pd10	4*i*	0.7347(7)	0	0.1443(8)	1
Pd11	4*e*	1/4	1/4	0	1
Pd12	8*j*	0.2966(3)	0.244(2)	0.2751(5)	1
Pd13	8*j*	0.1284(3)	0.230(2)	0.1799(4)	1
Pd14	8*j*	0.1639(3)	0.245(2)	0.4516(4)	1
Pd15	8*j*	0.4436(3)	0.245(3)	0.0634(4)	1
Pd16	8*j*	0.4874(3)	0.238(2)	0.3847(4)	1

97.9(4) % of $Lu_{10}Pd_{21}$, 2.1(1) % of Lu_3Pd_5

$Lu_{10}Pd_{21}$: a = 24.0474(2) Å, b = 5.66923(4) Å, c = 16.1400(1) Å, β = 91.8031(2)°

Lu_3Pd_5: a = 9.010(2) Å, b = 7.004(1) Å, c = 9.342(1) Å

$R_B(Lu_{10}Pd_{21})$ = 1.3 %, $R_F(Lu_{10}Pd_{21})$ = 1.6 %, B_{over} = 0.4735(2) Å^2

$R_B(Lu_3Pd_5)$ = 3.3 %, $R_F(Lu_3Pd_5)$ = 2.6 %, B_{over} = 0.800(4) Å^2

R_{wp} = 7.0 %, χ^2 = 1.3

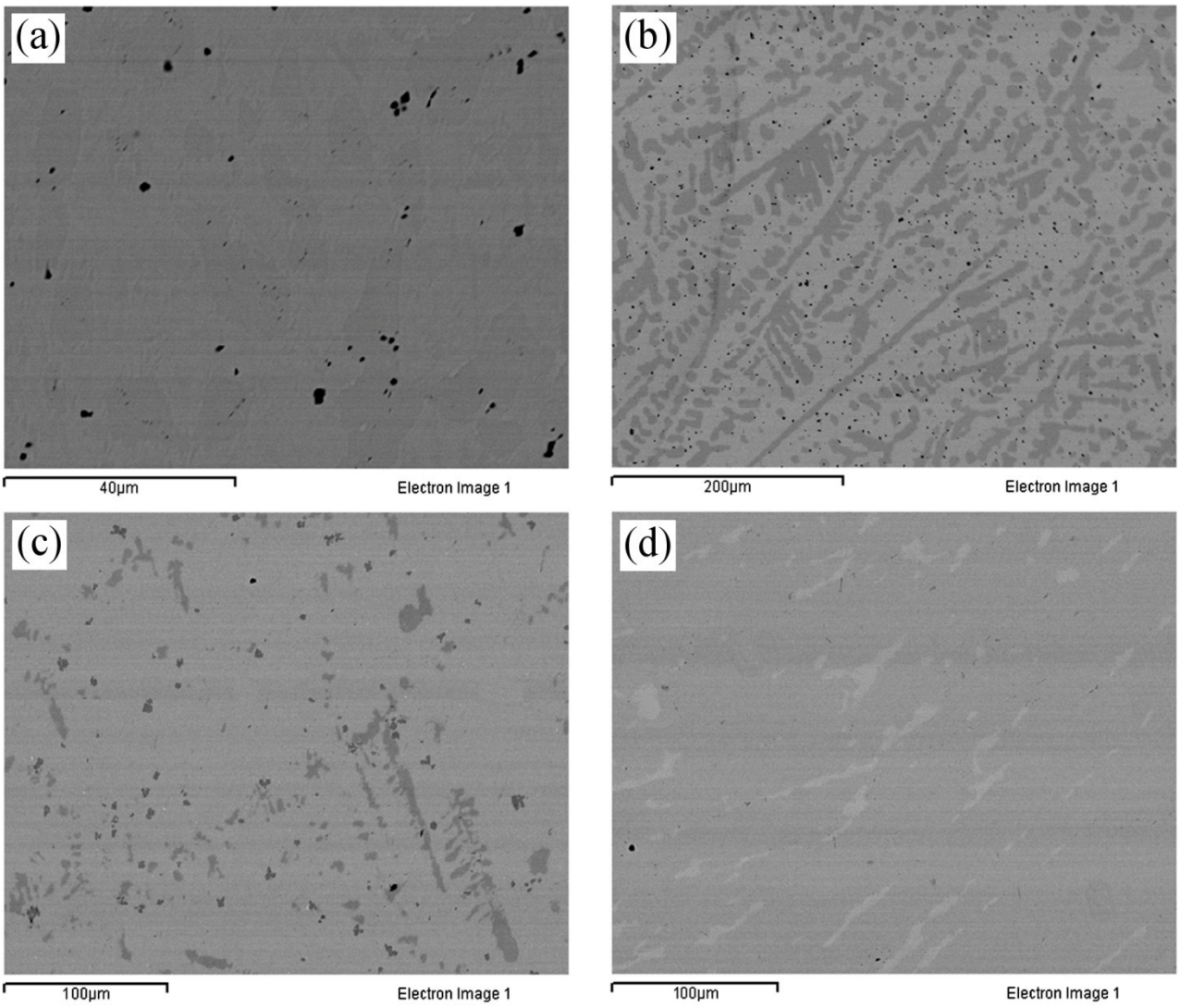

Fig. S1 SEM images [backscattered electron (BSE) mode] showing the microstructure in selected zones of four samples prepared at the compositions $Sc_{35}Pd_{65}$ (a), $Pr_{10}Pd_{21}$ (b), $Nd_{10}Pd_{21}$ (c) and $Gd_{10}Pd_{21}$ (d). In $Sc_{35}Pd_{65}$ sample the primary slightly darker grains are Sc_3Pd_5 and the matrix is a $ScPd_2$ phase. In $Pr_{10}Pd_{21}$ sample the darker primary dendritic grains are the $PrPd_3$ phase, while the lighter matrix is the new compound Pr_4Pd_7. In $Nd_{10}Pd_{21}$ sample the dark primary grains pertain to the $NdPd_3$ phase, while the lighter matrix is the $Nd_{10}Pd_{21}$ phase. In $Gd_{10}Pd_{21}$ sample the lighter grains are of Gd_3Pd_4 and the darker matrix is $Gd_{10}Pd_{21}$.

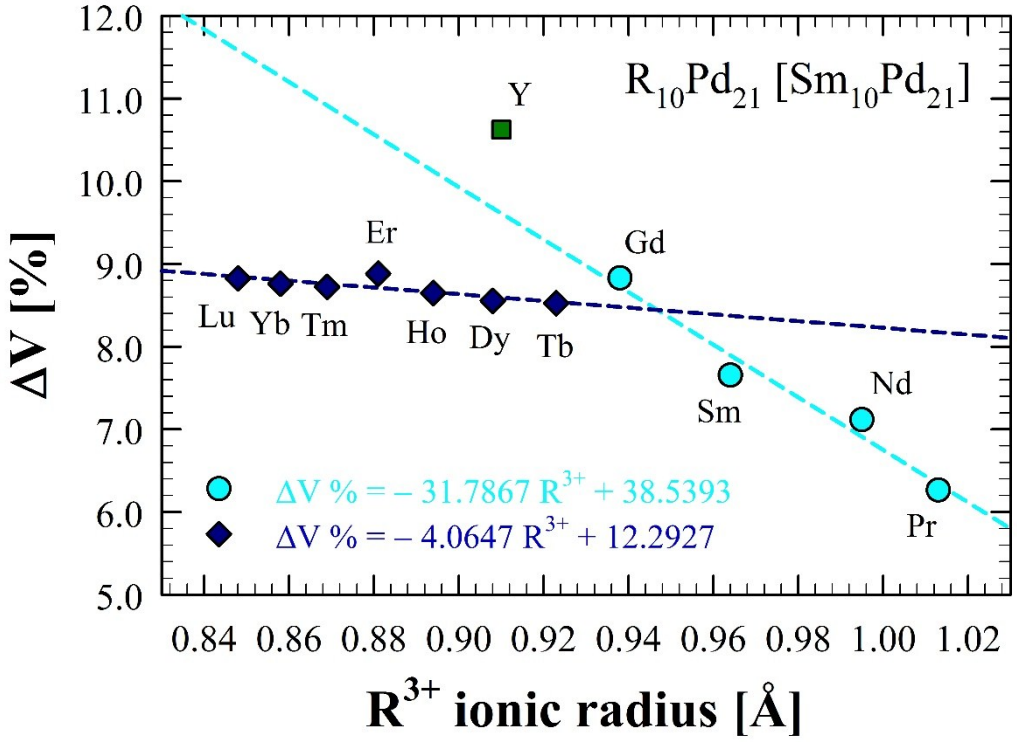

Fig. S2 Trend of the volume contraction (ΔV %) *vs.* the R^{3+} ionic radius for the $R_{10}Pd_{21}$ compounds.

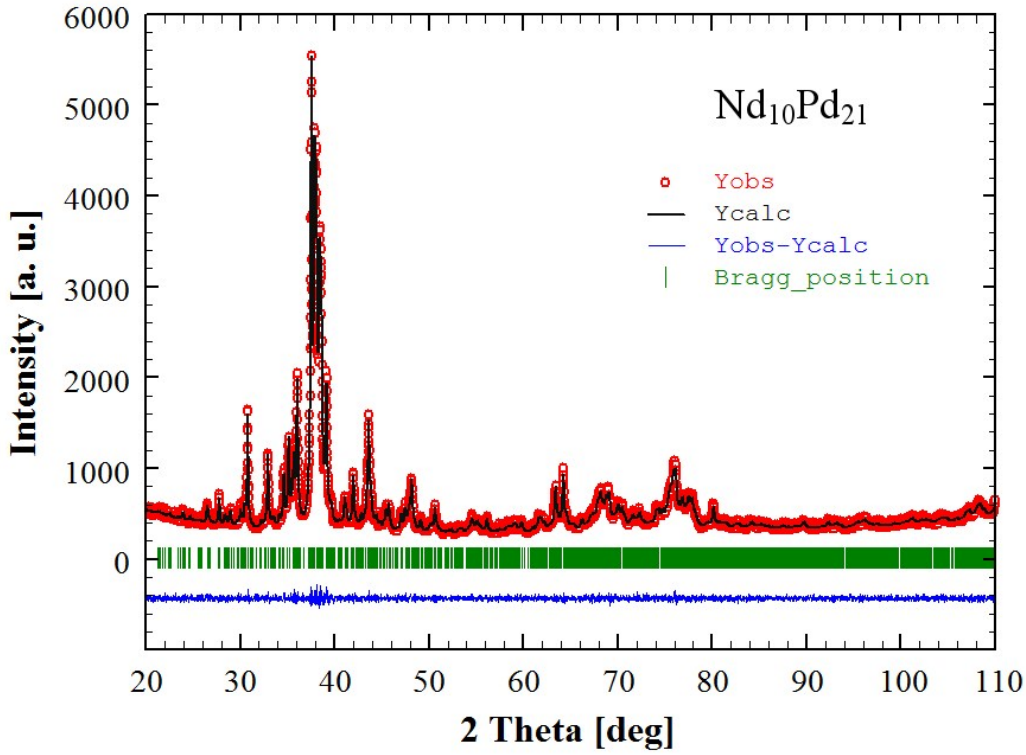

Fig. S3 Observed X-ray powder pattern (red circle) and Rietveld refinement profile (black line) for the $Nd_{10}Pd_{21}$ sample. The lower profile (blue line) gives the difference between observed and calculated data; the Bragg angle positions are indicated by vertical bars (green).

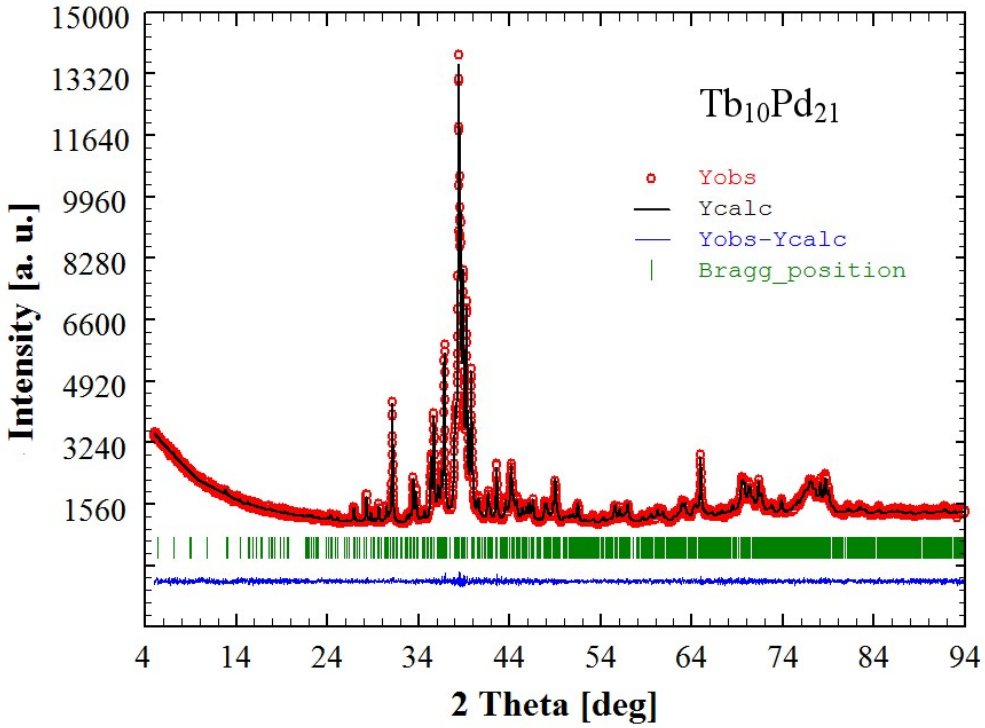

Fig. S4 Observed X-ray powder pattern (red circle) and Rietveld refinement profile (black line) for the $Tb_{10}Pd_{21}$ sample. The lower profile (blue line) gives the difference between observed and calculated data; the Bragg angle positions are indicated by vertical bars (green).

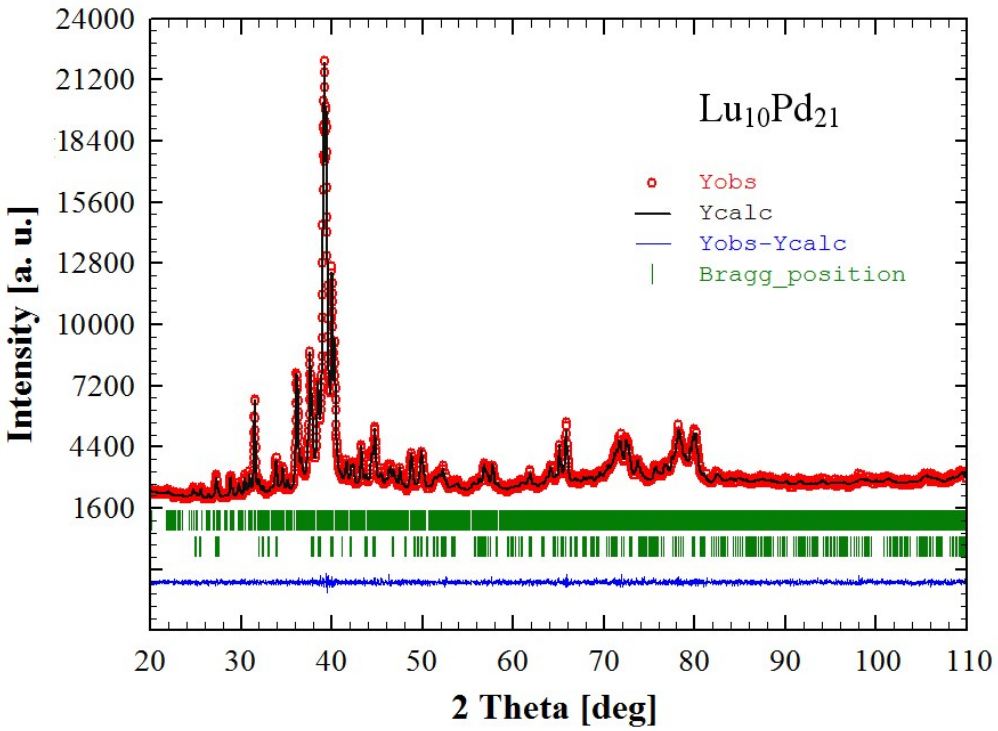

Fig. S5 Observed X-ray powder pattern (red circle) and Rietveld refinement profile (black line) for the $Lu_{10}Pd_{21}$ sample. The lower profile (blue line) gives the difference between observed and calculated data; the Bragg angle positions of the $Lu_{10}Pd_{21}$ (top) and $LuPd_3$ (bottom) phases are indicated by vertical bars (green).